

UC Irvine

UC Irvine Previously Published Works

Title

NHE3 Regulatory Factor 1 (NHERF1) Modulates Intestinal Sodium-dependent Phosphate Transporter (NaPi-2b) Expression in Apical Microvilli*

Permalink

<https://escholarship.org/uc/item/7hn539xs>

Journal

Journal of Biological Chemistry, 287(42)

ISSN

0021-9258

Authors

Giral, Hector

Cranston, DeeAnn

Lanzano, Luca

et al.

Publication Date

2012-10-01

DOI

10.1074/jbc.m112.392415

Supplemental Material

<https://escholarship.org/uc/item/7hn539xs#supplemental>

Copyright Information

This work is made available under the terms of a Creative Commons Attribution License, available at <https://creativecommons.org/licenses/by/4.0/>

Peer reviewed

NHE3 Regulatory Factor 1 (NHERF1) Modulates Intestinal Sodium-dependent Phosphate Transporter (NaPi-2b) Expression in Apical Microvilli*[§]

Received for publication, June 15, 2012, and in revised form, August 15, 2012. Published, JBC Papers in Press, August 17, 2012, DOI 10.1074/jbc.M112.392415

Hector Giral^{†1}, DeeAnn Cranston^{†1}, Luca Lanzano^{§1}, Yupanqui Caldas[‡], Eileen Sutherland[‡], Joanna Rachelson[‡], Evgenia Dobrinskikh[‡], Edward J. Weinman[¶], R. Brian Doctor[‡], Enrico Gratton[§], and Moshe Levi^{‡2}

From the [†]Department of Medicine, University of Colorado Denver, Aurora, Colorado and the Veterans Affairs Eastern Colorado Health Care System, Denver, Colorado 80045, the [§]Department of Biomedical Engineering, Laboratory for Fluorescence Dynamics, University of California, Irvine, California 92697, and the [¶]Department of Medicine and Department of Physiology, University of Maryland School of Medicine, Baltimore, Maryland 21201

Background: The type 2b sodium-dependent phosphate co-transporter (NaPi-2b) is the main mediator of intestinal active P_i absorption.

Results: NaPi-2b interacts with the PDZ domain of NHERF1 regulatory factor 1 (NHERF1).

Conclusion: NHERF1 is an important regulator of NaPi-2b apical membrane targeting in response to a low P_i diet.

Significance: Understanding of NaPi-2b adaptive mechanisms can help to design new therapies against hypo- and hyperphosphatemic disorders.

P_i uptake in the small intestine occurs predominantly through the NaPi-2b (SLC34a2) co-transporter. NaPi-2b is regulated by changes in dietary P_i but the mechanisms underlying this regulation are largely undetermined. Sequence analyses show NaPi-2b has a PDZ binding motif at its C terminus. Immunofluorescence imaging shows NaPi-2b and two PDZ domain containing proteins, NHERF1 and PDZK1, are expressed in the apical microvillar domain of rat small intestine enterocytes. Co-immunoprecipitation studies in rat enterocytes show that NHERF1 associates with NaPi-2b but not PDZK1. In HEK co-expression studies, GFP-NaPi-2b co-precipitates with FLAG-NHERF1. This interaction is markedly diminished when the C-terminal four amino acids are truncated from NaPi-2b. FLIM-FRET analyses using tagged proteins in CACO-2_{BBE} cells show a distinct phasor shift between NaPi-2b and NHERF1 but not between NaPi-2b and the PDZK1 pair. This shift demonstrates that NaPi-2b and NHERF1 reside within 10 nm of each other. NHERF1^{-/-} mice, but not PDZK1^{-/-} mice, had a diminished adaptation of NaPi-2b expression in response to a low P_i diet. Together these studies demonstrate that NHERF1 associates with NaPi-2b in enterocytes and regulates NaPi-2b adaptation.

Phosphate (P_i) is a key component of biological systems involved in a variety of physiologic processes including energy metabolism, cell signaling, nucleotide and phospholipids biosynthesis, and bone mineralization (1). Serum P_i levels are

maintained within a narrow range and deviation from these levels has significant pathological consequences. Hypophosphatemia leads to rickets and brittle bones in a number of inherited syndromes (2, 3), whereas hyperphosphatemia leads to increased morbidity and mortality from cardiovascular diseases (4–6). P_i homeostasis reflects the balance between intestinal absorption, renal reabsorption, deposition in bone, and cellular uptake.

The type II family of sodium-dependent phosphate co-transporters (NaPi) plays key roles in both the kidney and the small intestine. In the renal proximal tubule, NaPi-2a (SLC34a1) and NaPi-2c (SLC34a3) are expressed in the apical membrane of the proximal tubule where they perform the bulk of the renal P_i reabsorption. Both renal transporters are regulated in response to chronic and acute changes in dietary P_i content, metabolic conditions, and hormones, including parathyroid hormone and fibroblast growth factor 23 (FGF23) (7–9). Enterocyte transcellular absorption of luminal P_i is mainly mediated by the NaPi-2b (SLC34a2) co-transporter. Studies in NaPi-2b³ KO mice indicate that NaPi-2b contributes to ~90% of active P_i absorption in the ileum (10). Similar to the renal adaptation of NaPi-2a and NaPi-2c, NaPi-2b activity is regulated in response to both acute and chronic changes in dietary P_i intake (11, 12). Mice chronically fed a low P_i diet have an increased apical expression of NaPi-2b transporter in enterocytes and an up-regulation of P_i uptake (13).

Significant advances in delineating the molecular and cellular mechanisms underlying the regulation of the renal transporters, especially NaPi-2a, have been made over the last decade. The primary mechanism of regulating NaPi-2a and

* This work was supported, in whole or in part, by National Institutes of Health Grants R01 DK066029-6 (to M. L., E. G., H. G., Y. C., and L. L.), R01 DK-080769 (to B. D., D. C., J. R., and E. D.), 8P41GM103540 (to E. G. and L. L.), and P50-GM076516 (to E. G. and L. L.).

[§] This article contains supplemental Figs. S1–S4.

¹ These authors contributed equally to this work.

² To whom correspondence should be addressed: Div. of Renal Diseases & Hypertension, University of Colorado-Denver, 12700 East 19th Ave., Research 2, Rm. 7002, Box C281, Aurora, CO 80045. Tel.: 303-724-4825; Fax: 303-724-4868; E-mail: Moshe.Levi@ucdenver.edu or MMJL@AOL.COM.

³ The abbreviations used are: NaPi-2b, sodium-dependent phosphate co-transporter type 2b; NHERF1, NHE3 regulatory factor 1; PDZK1, PDZ domain-containing protein in kidney 1; FLIM, fluorescence lifetime imaging microscopy; FRET, Förster resonance energy transfer; KO, knock-out; BBM brush-border membrane.

NaPi-2b Transporter Interacts with the PDZ Protein NHERF1

NaPi-2c activity is via modulation of the abundance of NaPi protein in the apical membrane of proximal tubule cells (14, 15). The interactions of NaPi-2a and NaPi-2c with PDZ (PSD-95, Dlg, ZO-1) domain-containing proteins play pivotal roles in directing the retention *versus* recovery of these transporters at the apical membrane.

PDZ is one of the most extended protein-protein interaction domains found in mammalian proteins involved in an increasing number of cellular functions including the regulation of epithelial transporters (16, 17). PDZ domains are modules consisting of 80–100 amino acid residues that generate a hydrophobic pocket that is able to fit specific sequences (PDZ-binding motifs), usually located at the C-terminal tail of many proteins (18). NaPi-2a binds and is regulated by several PDZ proteins, including NHERF1 (also known as EBP50), NHERF-2 (also known as E3KARP), PDZK1 (also known as NHERF-3, CAP70, NaPi-Cap1), PDZK2 (also known as NHERF-4, NaPi-Cap2), and Shank2 (19–21). However, NaPi-2c interactions have only been demonstrated with PDZK1 and, to a lesser extent, with NHERF1 (22, 23).

Highlighting the functional significance of these interactions, NHERF1^{-/-} mice have a marked redistribution of NaPi-2a from the apical microvilli into the cell interior and distinct increased urinary P_i excretion that results from the loss of NaPi-2a activity in the renal proximal tubule cells (24). PDZK1^{-/-} mice showed milder effects on the regulation of NaPi-2a only under high P_i diet adaptation with lower levels of protein, paralleled with increased urinary fractional P_i excretion (25). However, the up-regulation of NaPi-2c apical protein in response to a low P_i diet was blunted in the PDZK1^{-/-} mice, suggesting an important role of PDZK1 on the stabilization of NaPi-2c (23).

In contrast to regulation of renal P_i transport, the regulatory mechanisms controlling the intestinal absorption of P_i have not been studied in detail and are still largely unknown. Interestingly, intestinal NaPi-2b transporter contains a PDZ-binding motif consensus sequence at its C terminus, but at the present time no reports have described its interactions with PDZ proteins. Given the established role of NHERF1 and PDZK1 in binding and moderating the activity of other NaPi type II family members, the present study seeks to determine whether NHERF1 and PDZK1 bind and modulate the activity of NaPi-2b in small intestinal enterocytes.

EXPERIMENTAL PROCEDURES

Materials and Antibodies—All chemicals were obtained from Sigma except when noted. The polyclonal rabbit anti-NaPi-2b antibody was custom generated by Davids Biotechnologie (Regensburg, Germany) as described before (12). NHERF1 rabbit polyclonal antibody (Abcam, Cambridge, MA) and PDZK1 mouse monoclonal (BD, Franklin Lakes, NJ) and goat polyclonal (Santa Cruz Biotechnology, Santa Cruz, CA) antibody were commercially available.

Animal Procedures and Diets—Male Sprague-Dawley rats (8–10-week-old, 200–250 g body weight; Harlan, Madison, WI) were used for the isolation of rat enterocytes and immunofluorescence localization studies. P_i dietary adaptation was performed in PDZK1^{-/-} mice (26), NHERF1^{-/-} mice (24), and

age- and sex-matched wild type control mice were obtained from The Jackson Laboratories (Bar Harbor, ME). The animals were maintained on a 12-h light/12-h dark cycle and normal drinking water was supplied *ad libitum*. The mice were acclimated on regular chow diet and then fed *ad libitum* a high P_i (1.5% P_i, diet TD.08499) or a low P_i (0.1% P_i, diet TD.85010) diet (Harlan Teklad) for 7 days. The diets were otherwise matched for their calcium (0.6%), magnesium, sodium, protein, fat, and vitamin D content. A total of 24 mice for each experimental group were studied. The animal study protocols were approved by the Animal Care and Use Committee at the University of Colorado-Denver.

Isolation of Rat Enterocytes—Enterocytes were isolated from the duodenum of rats. Briefly, rats were euthanized (70 mg/kg of pentobarbital). The small intestine was excised and flushed with PBS. The initial 10 cm of small intestine was separated and cut along its length to expose the lumen. This segment was placed in 10 ml of Enterocyte Isolation Buffer (Dulbecco PBS, 15 mM HEPES, 1 mM EDTA, 100 mM *N*-acetylcysteine), rotated vigorously at 37 °C for 15 min, vortexed for 15 s, the suspension poured through cheesecloth, the resultant suspension was placed on ice and the process was repeated. The isolated enterocytes were then washed twice in PBS.

Co-immunoprecipitation of Native NaPi-2b and NHERF1—Isolated rat enterocytes were lysed in RIPA buffer (50 mM Tris, pH 7.6, 150 mM NaCl, 5 mM EDTA, 0.5% Triton X-100, 0.5% Nonidet P-40, 0.1% SDS, 0.1% sodium deoxycholate) supplemented with HALT protease and phosphatase inhibitors (Thermo Scientific, Rockford, IL), and solubilized at 25 °C for 40 min. A total cell lysate sample was removed and the insoluble material was pelleted at 12,000 × *g* for 10 min. The resulting supernatant was pre-cleared with Ultralink Immobilized Protein A/G Plus beads (Pierce) for 1 h at 4 °C. 10 μg of either NaPi-2b rabbit polyclonal antibody, NHERF1 mouse monoclonal antibody (Abcam, Cambridge, MA), or goat polyclonal PDZK1 (Santa Cruz Biotechnology) was bound with 150-μl Ultralink Protein A/G beads for 1 h at room temperature. Beads bound with antibody were rinsed with RIPA buffer and incubated with pre-cleared supernatant overnight at 4 °C. Pre-clear and immunoprecipitation beads were washed 3 times with RIPA buffer and eluted with 5× PAGE solution (5% SDS, 25% sucrose, 50 mM Tris, 5 mM EDTA, pH 8). Immunoprecipitated proteins were analyzed via Western blot analysis.

Co-immunoprecipitation of FLAG-NHERF1 and GFP-NaPi-2b—HEK-293 cells were co-transfected with FLAG-NHERF1 and either full-length or truncated GFP-NaPi-2b. In truncated GFP-NaPi-2b (GFP-NaPi-2b-4aa), the last four amino acids were deleted using site-directed mutagenesis as directed by the manufacturer (Agilent Technologies, Santa Clara, CA). The primers used to create the mutant were: forward, AGGCCCTGTCCAAGTGGGGCACCTAGG; reverse, CCTAGGTGCCCTAGTTGGACAGGGCCT. HEK-293 cells were grown in DMEM supplemented with 10% FBS, penicillin, streptomycin, and L-glutamine at 37 °C with 5% CO₂. At ~80% confluence, cells were transfected using Lipofectamine 2000 as directed by the manufacturer (Invitrogen). After 48 h of co-expression, cells were harvested in FLAG lysis buffer (150 mM NaCl, 50 mM Tris, 1 mM EDTA, 1% Triton X-100, pH 7.4; HALT protease

inhibitors (Thermo Scientific)). Insoluble material was pelleted at $12,000 \times g$ for 10 min. After washing in FLAG lysis buffer, FLAG-tagged agarose beads (Sigma) were added to the resulting supernatant and incubated overnight at 4 °C. The beads were rinsed 3 times with FLAG lysis buffer and eluted with 5× PAGE solution (5% SDS, 25% sucrose, 50 mM Tris, 5 mM EDTA, pH 8). Immunoprecipitated proteins were analyzed via Western blot analysis.

Brush-Border Membrane Vesicles Isolation—Ileum brush-border membrane vesicles were isolated by a double Mg^{2+} precipitation technique as described before (12, 27) with slight variations. Ileal mucosal scrapes (corresponding to the distal 15 cm of the small intestine) from two mice were combined in 15 ml of isolation buffer consisting of 50 mM mannitol, 2 mM HEPES/NaOH, pH 7.1, and Complete protease inhibitor (Roche Diagnostics). Ileal mucosa samples were homogenized with a Potter-Elvehjem homogenizer. Brush-border membrane vesicles were prepared by a double serial Mg^{2+} precipitation procedure. First, $MgCl_2$ was added to the homogenates (13 mM final concentration), incubated on ice for 20 min, and centrifuged at $3,000 \times g$. The supernatant was centrifuged at $38,000 \times g$ at 4 °C for 40 min. The second Mg^{2+} precipitation step was performed by resuspending the membrane pellet in 7.5 ml of solution B (300 mM mannitol, 0.1 mM $MgSO_4$, 20 mM HEPES/NaOH, pH 7.1, and Complete protease inhibitor) with a 20-gauge needle. The samples were centrifuged at $6,000 \times g$ and the supernatant was transferred to a clean tube. Final centrifugation at $38,000 \times g$ at 4 °C for 40 min resulted in a pellet containing an ileal brush-border membrane vesicle that was resuspended in final buffer (300 mM mannitol, 16 mM HEPES/Tris, pH 7.5, and Complete protease inhibitor) by passing through a 25-gauge needle.

Western Blot Analysis—Ileal brush-border membrane vesicle samples or proteins from rat immunoprecipitation were separated in 10% SDS-PAGE gels and transferred onto nitrocellulose membranes (Bio-Rad). The membranes were blocked with 5% milk in PBS with 0.1% Tween 20 (PBST; 80 mM Na_2HPO_4 , 25 mM NaH_2PO_4 , 100 mM NaCl, and 0.1% Tween 20, pH 7.5) before incubation with primary antibodies overnight at 4 °C. The primary antibodies used included: rabbit polyclonal against NaPi-2b (Davids Biotechnologie, Germany), rabbit polyclonal antibody against NHERF1 (EBP50) (Abcam), polyclonal against PDZK1, rabbit polyclonal antibody against Galectin-4 (Invitrogen), rabbit polyclonal antibody against SGLT1 (Alpha Diagnostics, San Antonio, TX), and mouse monoclonal against β -actin (Sigma). The membranes were incubated with HRP-linked secondary antibodies for 1 h followed for several washes with PBST. The membranes were incubated with SuperSignal West Pico Chemiluminescent Substrate (Thermo Scientific). Images were acquired and analyzed by densitometry using a Biospectrum 500 imaging system (UVP).

Cell Culture and Transfection—The CACO₂_{BBE} clone was kindly provided by Mark Mooseker (28). CACO₂_{BBE} cells were grown in DMEM supplemented with 20% fetal bovine serum, penicillin, streptomycin, and L-glutamine at 37 °C and 5% CO₂ incubator. Transfections were achieved with Lipofectamine 2000 (Invitrogen) and cells at 90% confluence, following the

manufacturer's instructions. CACO₂_{BBE} cells expressing the fluorescent fusion proteins were grown on collagen-coated eight-well Lab-Tek chambered coverglass (Nunc). Measurements were performed 24–48 h after transfection.

FLIM-FRET Microscopy—Fluorescence lifetime imaging microscopy (FLIM) measurement of Förster resonance energy transfer (FRET) was performed using a Zeiss LSM 510 microscope (Jena, Germany) equipped with a FLIMBox, a digital frequency-domain setup capable of multiharmonic analysis (29). The setup and imaging procedure has been extensively detailed before (23). Briefly, images of the cell apical membrane were obtained in the 256×256 format with a pixel dwell time of 25.6 μ s/pixel and averaging over 20 frames. SimFCS software was used for the acquisition and analysis of FLIM images following the phasor analysis (23). Briefly, we used our digital frequency-domain setup to measure the modulation and phase at each of the pixels of an image. The modulation and phase are used to determine, respectively, the radial and angular coordinate of the phasor in a polar plot (31). The phasor associated to each cell imaged with FLIM was determined as the average phasor of the pixels corresponding to the cell apical membrane. In each experiment we determined the phasors of the unquenched donor (D_{unq}) as the average phasor of cells transfected only with Cerulean (Cu)-NaPi-2b, the phasor of the donor-acceptor pair (D+A) as the average of cells transfected with Cu-NaPi-2b and EYFP-NHERF1 or EYFP-PDZK1, and phasor of the autofluorescence by imaging nontransfected cells.

FRET Analysis in the Phasor Plot—To quantify FRET results we analyzed the shift of the phasor of the donor in the presence of the acceptor with respect to the donor only. The trajectory of variable FRET efficiency is drawn in the plot starting from the donor only position ($E = 0$) to the autofluorescence phasor position ($E = 1$) (supplemental Fig. S1). Any phasor along this trajectory corresponds to a pure species of donor quenched (D_q) with FRET efficiency E . If the donors are not all paired with an acceptor, then a pixel may contain a mixture of quenched and unquenched donors with relative fractions f_q and f_{unq} , respectively. In this case the phasor corresponding to donor plus acceptor (D+A) is a normalized linear combination of the phasors of D_q and D_{unq} and lies along the line connecting the two phasors. The fraction of interacting donors, f_q , in a given mixture can be calculated from the distance of the phasor D+A from D_{unq} divided by the length of the entire segment (supplemental Fig. S1).

In our experiments, the phasors of donor-acceptor cells (D+A) were described by a linear combination of quenched and unquenched donor species. The quenched donor (D_q) position has been extrapolated at the intersection between a linear fit of the data and the efficiency trajectory as described previously (23). The position of D_q yields the value of efficiency E associated with the FRET interaction and represents the maximum FRET detectable if all the donors were ideally paired with an acceptor. To calculate the fraction of quenched donors, f_q , associated to each phasor we considered the projection of the phasor on the linear fit and then divided its distance from D_{unq} by the length of the segment connecting D_q and D_{unq} .

Modulation Tracking of Microvilli—The modulation tracking images were obtained using a customized microscope at the

NaPi-2b Transporter Interacts with the PDZ Protein NHERF1

Laboratory for Fluorescence Dynamics. The principle of the technique and methodology details has been already described in detail (32). A Chameleon Ultra II laser (Coherent, CA) tuned at 930 nm was used for 2-photon excitation of enhanced green fluorescent protein or enhanced yellow fluorescent protein. A schematic of the modulation tracking imaging method is shown in supplemental Fig. S2. First a raster scan of the apical membrane is performed (supplemental Fig. S2A). Then we choose one isolated microvillus and point the scanner on its coordinates. We then start the tracking routine by scanning the laser spot in a circular orbit around the microvillus at any given section while scanning along its length to obtain a three-dimensional image of the surface in one or two channels (supplemental Fig. S2B). By modulation tracking, we obtain three-dimensional reconstructions of the microvilli surface (Fig. 4). The three-dimensional reconstruction is painted in color scale according to the fluorescence intensity recorded in one channel.

Statistical Analysis—Data are expressed as mean \pm S.E.; *, $p < 0.05$; **, $p < 0.005$; and ***, $p < 0.001$. Data were analyzed for statistical significance by unpaired Student's *t* test or one-way analysis of variance.

RESULTS

NaPi-2b Has a PDZ Binding Motif on the C-terminal Tail—Many of the PDZ domain containing proteins that have documented within the apical membrane of epithelial cells are type I domains. This includes NHERF1 and PDZK1. Type I PDZ domains bind to the C-terminal tails of proteins with consensus sequences of $-X-T/S-X-\Phi$ (Φ = hydrophobic amino acid). Sequence analysis showed that NaPi-2b presents a well conserved PDZ-binding site at its C terminus end. The C-terminal sequence of NaPi-2b in both mice (accession NP_035532.2) and rats (accession NP_445832.1) is T-T-V-F. The C-terminal sequence of NaPi-2b in human (accession AAI46667.1) is C-T-A-L. Although there is divergence in the absolute sequence, the C-terminal sequence of NaPi-2b across species has retained its canonical PDZ binding motif. Consequently, the present studies were performed to test the hypothesis that PDZ domain containing proteins bind and regulate NaPi-2b.

NaPi-2b, NHERF1, and PDZK1 Are All Expressed in Enterocyte Microvilli—NHERF1 and PDZK1 have an established history of regulating key transport proteins within the apical membrane of a variety of epithelial cell types, including enterocytes (17, 33). Western blotting reconfirms that, in control rats, NaPi-2b and both PDZ domain containing proteins are expressed in rat enterocytes (Fig. 1A). NaPi-2b expression was greatest in the rat duodenum and jejunum segments with lesser amounts seen in the ileum. NHERF1 and PDZK1 were expressed with relative equal abundance in all three intestinal segments. Staining of rat duodenum segments with phalloidin highlighted the apical microvilli on the enterocytes. Immunofluorescence imaging of NaPi-2b, NHERF1, and PDZK1 showed that all three proteins were expressed within the apical microvilli domain, putting each of the PDZ domain containing proteins in approximate position to interact with NaPi-2b (Fig. 1B).

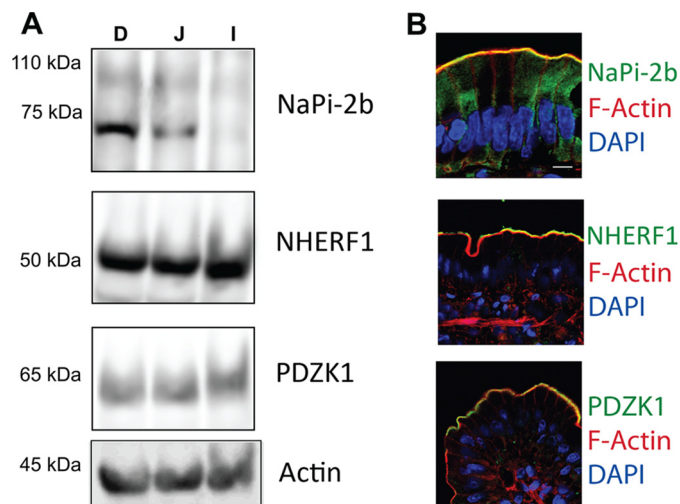


FIGURE 1. NaPi-2b, NHERF1, and PDZK1 are expressed in the enterocyte microvilli. A, isolated rat enterocytes analyzed by Western blot showed expression in the small intestine of the proteins under study. NaPi-2b expression was greater in the duodenum followed by jejunum and negligible levels on the ileal section. Both NHERF1 and PDZK1 proteins showed similar expression levels in all three segments. B, immunofluorescence microscopy of rat duodenal sections demonstrated that NaPi-2b, NHERF1, and PDZK1 (green) are expressed in the apical membrane of enterocytes, co-localizing with the actin signal (red) in the microvilli. Bar, 10 μ m.

NaPi-2b Binds with NHERF1—The potential association between either NHERF1 or PDZK1 and NaPi-2b in duodenal enterocytes was evaluated by co-immunoprecipitation. Enterocyte lysates were initially pre-cleared to remove proteins with significant binding to the protein A/G beads. No appreciable levels of any of the proteins being studied were observed in the pre-clear samples (Fig. 2). Following the immunoprecipitation of NHERF1, Western blotting of the precipitated fraction showed both NHERF1 and NaPi-2b were present (Fig. 2). In contrast, following immunoprecipitation of PDZK1, Western blotting of the immunoprecipitates demonstrated the presence of PDZK1 but failed to detect the co-precipitation of NaPi-2b (Fig. 2). When subjecting enterocyte lysates to immunoprecipitation of NaPi-2b, interference of the IgG bands precluded the confirmation that NaPi-2b was precipitated. Western blotting of the precipitated fractions did, however, demonstrate the presence of NHERF1 but not PDZK1 (Fig. 2). Taken together, these studies did not observe any appreciable co-precipitation between NaPi-2b and PDZK1 but readily demonstrated co-precipitation of NaPi-2b and NHERF1. This indicates NaPi-2b and NHERF1 reside within a common protein complex in native rat enterocytes.

The association between NaPi-2b and NHERF1 was further examined in HEK co-transfection/co-precipitation studies. GFP-NaPi-2b was readily detected in the FLAG co-immunoprecipitated fraction in HEK cells co-transfected with GFP-NaPi-2b and FLAG-NHERF1 (supplemental Fig. S3). To determine whether the putative PDZ binding motif of NaPi-2b promotes the binding interaction with NHERF1, co-precipitation of GFP-NaPi-2b with FLAG-NHERF1 was compared between full-length GFP-NaPi-2b and GFP-NaPi-2b with four amino acids truncated from the C-terminal tail (GFP-NaPi-2b-4aa). Fluorescence imaging of co-transfected HEK cells showed that both GFP-NaPi-2b and GFP-NaPi-2b-4aa were localized

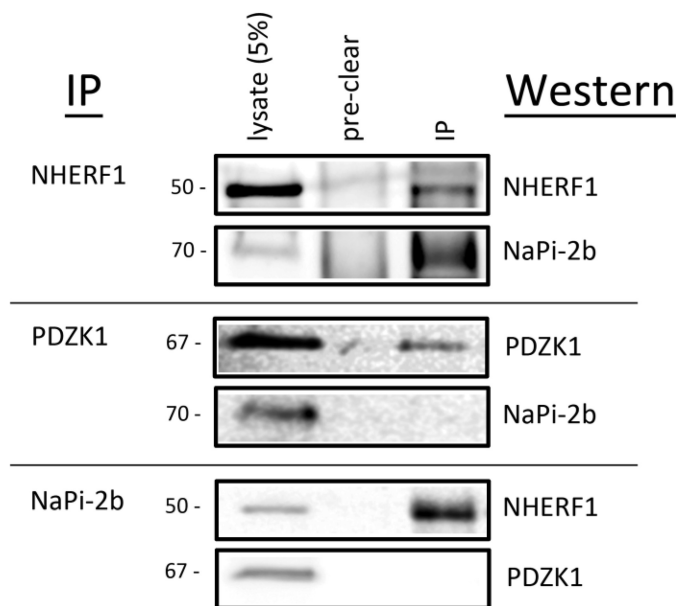


FIGURE 2. NaPi-2b associates with NHERF1 in rat duodenal enterocytes. Rat duodenal enterocyte lysates were subjected to immunoprecipitation (IP) and Western blot analysis of co-precipitating proteins. No appreciable levels of any of the proteins studied appeared within the protein A/G pre-cleared samples. In NHERF1 immunoprecipitates, NHERF1 was precipitated and NaPi-2b was readily detected in the immunoprecipitated sample (*top panel*). In PDZK1 immunoprecipitates, PDZK1 was precipitated but NaPi-2b was not observed in the immunoprecipitated sample (*middle panel*). In NaPi-2b immunoprecipitates, NHERF1 but not PDZK1 was found in immunoprecipitated samples (*bottom panel*). Interference of the IgG bands precluded the confirmation that NaPi-2b was precipitated in these samples.

predominantly at the plasma membrane and co-localized extensively with mCherry-NHERF1 (Fig. 3A). Lysates in all samples expressed approximately equivalent levels of either GFP-NaPi-2b or GFP-NaPi-2b-4aa. FLAG-NHERF1 was confirmed in cells that were co-transfected with FLAG-NHERF1 cDNA. Western blotting showed FLAG-NHERF1 was readily pulled out of the lysates from cells co-transfected with FLAG-NHERF1 cDNA. Minimal signal was detected in the FLAG precipitate fractions when GFP-NaPi-2b or GFP-NaPi-2b-4aa were expressed alone (Fig. 3B). When co-expressed with FLAG-NHERF1, GFP-NaPi-2b was readily detected in the FLAG co-immunoprecipitated fraction. In contrast, comparatively little GFP-NaPi-2b-4aa co-precipitated with FLAG-NHERF1 (Fig. 3B). These observations confirm the association between NaPi-2b and NHERF1 and indicate that the PDZ-binding motif of NaPi-2b plays a pivotal role in the interaction between NaPi-2b and NHERF1.

CACO-2_{BBE} Cells as an Enterocyte Cell Model to Study NaP_i Transporters—Despite its colonic cancer cell origin, CACO-2 cells express many characteristics of small intestine epithelial cells and it has been extensively used as a model of enterocyte transport function and regulation (34–37). The CACO-2_{BBE} clone was established for the study of actin cytoskeleton architecture and presents typical epithelial polarity characterized by robust microvilli formation (38, 39).

CACO-2_{BBE} cells were used to further confirm the interactions of NaPi-2b with PDZ proteins in a live enterocyte cell model. Confocal microscopy of transfected CACO-2_{BBE} cells showed that EYFP-NaPi-2b (Fig. 4A), as well as EYFP-NHERF1

and EYFP-PDZK1 (data not shown), were concentrated within the apical membrane domain. Moreover, modulation tracking microscopy demonstrated that all three proteins reside within individual microvilli (Fig. 4B). Co-transfected CACO-2_{BBE} cells were subsequently utilized in FLIM-FRET studies to determine whether NaPi-2b interacted with either NHERF1 or PDZK1 within microvilli.

FLIM-FRET Analysis of NaPi-2b and NHERF1 Interactions in CACO-2_{BBE} Cells—To determine FRET occurrence we performed fluorescent lifetime imaging (FLIM-FRET) measurements of the donor fluorophore (cerulean or Cu). The FLIM data were analyzed and interpreted using the phasor analysis as described under “Experimental Procedures” (40). FRET occurrence is observed in the phasor plot as a shift that depends on the efficiency of the interaction and the fraction of molecules undergoing FRET.

Fig. 5 shows representative images of CACO-2_{BBE} cells transfected either with only the donor (D) species Cu-NaPi-2b (Fig. 5A) or with both donor and acceptor (D+A) species Cu-NaPi-2b and EYFP-NHERF1, respectively (Fig. 5B). Using the FLIM measurements, the average phasor position of D in the phasor plot was determined and compared with the phasors of D+A species (Fig. 5C). The phasors of cells co-transfected with NaPi-2b and NHERF1 are shifted toward the direction of lower lifetimes showing the occurrence of FRET. FRET can only occur when the donor (Cu-NaPi-2b) and acceptor (EYFP-NHERF1) species are localized within 10 nm of each other. The phasors associated with the D+A lifetime can be described as a linear combination of the phasors of two species: unquenched (unq) and quenched (q) donors with a given FRET efficiency (*E*). Further analysis of the phasor plot showed the fraction of donors undergoing FRET was 0.20 ± 0.02 and the FRET efficiency was 0.54 ± 0.01 ($n = 11$). FLIM-FRET analysis of NaPi-2b and PDZK1 in CACO-2_{BBE} cells was then evaluated. Fig. 5 shows confocal images of CACO-2_{BBE} cells expressing only Cu-NaPi-2b (Fig. 5D) and Cu-NaPi-2b and EYFP-PDZK1 (Fig. 5E), respectively. The experimental lifetime phasor associated to the cells co-transfected with Cu-NaPi-2b and EYFP-PDZK1 (D+A) is not significantly shifted with respect to the average phasor of the donor only (D) (Fig. 5F). The average position of the NaPi-2b/NHERF1 lifetime phasor was included to highlight the lack of FRET between NaPi-2b and PDZK1. The negative occurrence of FRET between NaPi-2b and PDZK1 indicates their associated fluorophores do not reside within 10 nm of each other.

Intestinal BBM NaPi-2b Protein Adaptation to a Low P_i Diet Is Impaired in NHERF1 KO Mice But Not in PDZK1 KO Mice—NHERF1^{-/-} mice were used to evaluate the relevance of NHERF1 in the regulation of NaPi-2b (24). In mice, intestinal uptake and NaPi-2b expression is greatest in the ileal segment of the small intestine (11). Brush border membrane (BBM) vesicles isolated from ileal enterocytes were analyzed by Western blot. In response to a low P_i diet, the apical expression of NaPi-2b is increased in NHERF1^{+/+} mice as previously reported (13, 41). However, NHERF1^{-/-} mice fed a low P_i diet showed diminished adaptive response compared with wild type animals with only partial up-regulation on the levels of apical NaPi-2b. Densitometric analysis of NaPi-2b levels in the apical

NaPi-2b Transporter Interacts with the PDZ Protein NHERF1

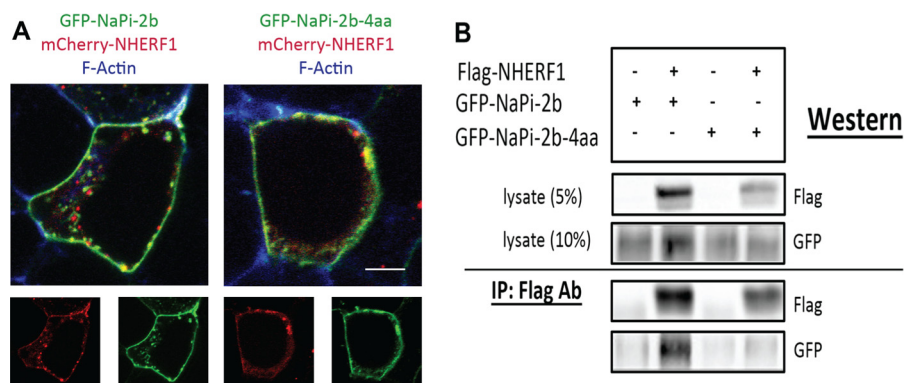


FIGURE 3. C-tail truncation impacts NaPi-2b binding to NHERF1. *A*, HEK cells were co-transfected with mCherry-NHERF1 and either GFP-NaPi-2b or GFP-NaPi-2b-4aa. Confocal fluorescence imaging shows that mCherry-NHERF1 co-localizes with both GFP-NaPi-2b and GFP-NaPi-2b-4aa. Each of the three proteins is distributed predominantly at the plasma membrane. *Bar*, 5 μm . *B*, HEK cells were transfected with GFP-NaPi-2b or GFP-NaPi-2b-4aa, either alone or with FLAG-NHERF1. In the *upper panel*, Western blotting of the total cell lysates showed similar expression levels of each protein. In the *lower panel*, Western blotting showed GFP-NaPi-2b, but not GFP-NaPi-2b-4aa, was readily co-precipitated with FLAG-NHERF1.

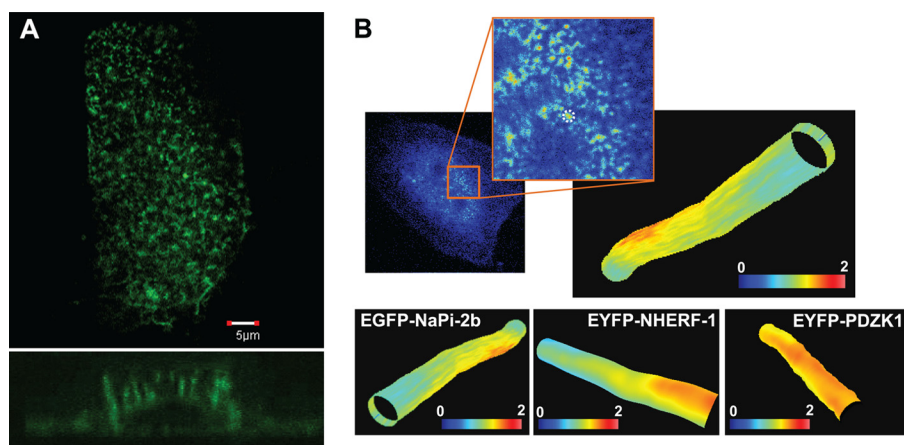


FIGURE 4. The enterocyte cell model CACO-2_{BBE} correctly expresses NaPi-2b, NHERF1, and PDZK1. *A*, immunofluorescence confocal microscopy of EYFP-NaPi-2b in transfected CACO-2_{BBE} cells showed that the transporter was correctly expressed in numerous microvilli on the apical membrane. *Lower panel* shows cross-section of a cell from the apical to the basolateral membrane. *B*, modulation tracking microscopy was used to image EYFP-NaPi-2b, EYFP-NHERF1, and EYFP-PDZK1 transfected in CACO-2_{BBE} cells. This technique allows us to track and scan individual microvilli of the apical membrane. Therefore we confirmed proper expression of all three proteins in the microvilli of CACO-2_{BBE} cells. Color scale represents fluorescence intensity.

membrane of NHERF1^{-/-} mice showed a reduction of 39 ± 11% of the response measured in wild type mice (Fig. 6). These results indicate that NHERF1 contributes to NaPi-2b adaptation in low P_i diet fed animals. In parallel we evaluated the expression of other apical proteins to evaluate if depletion of the NHERF1 protein would affect other membrane proteins in a general way. Both galectin-4 and Na(+)-D-glucose cotransporter (SGLT1) expression were not modified in NHERF1^{-/-} mice compared with wild type (Fig. 7).

In contrast to the loss of NaPi-2b adaptation measured in NHERF1^{-/-} mice, no change in adaptation was observed in PDZK1^{-/-} mice fed a low P_i diet (Fig. 8). Densitometric analysis of NaPi-2b levels in ileal BBM vesicles from PDZK1^{-/-} mice showed no differences to the levels measured in matched wild type controls.

DISCUSSION

PDZ Proteins Regulate Key Apical Transporters in Epithelial Cells—PSD95-Dlg-ZO-1 (PDZ) domains are ~90 amino acids in size and coordinate protein-protein binding interactions. There are over 400 distinct PDZ domain-containing proteins coded for in the human genome with expression of PDZ

domain containing proteins found in all cell types (18, 42). Because the initial characterization of the PDZ protein-protein binding module of ZO-1, PDZ domain-containing proteins have continued to emerge as pivotal proteins in moderating a variety of functions within distinct domains of epithelial cells (16, 17). This is specifically evidenced by the regulation of ion transporter and channel proteins within the apical membrane of epithelial cells. Two independent laboratories discovered a 50-kDa phosphoprotein bound to the actin-associated AKAP protein ezrin (termed ezrin-radixin-moesin binding phosphoprotein 50 or EBP50) and that also bound and regulated the sodium-proton exchanger 3 (NHE3) in the apical microvilli of renal proximal tubules (termed NHE3 regulatory factor 1 or NHERF1) (43–45). Upon confirming that EBP50 and NHERF1 were the same protein, other key epithelial transport proteins were found to bind with NHERF1 (19, 22, 46, 47).

PDZ Proteins Regulate NaPi-2 Family Members—The physiologic significance of NHERF1 in regulating epithelial sodium-dependent P_i transporters (NaPi) was highlighted in NHERF1 KO mice (24, 48). When compared with wild type littermates, NHERF1^{-/-} mice had lower serum P_i levels and significantly

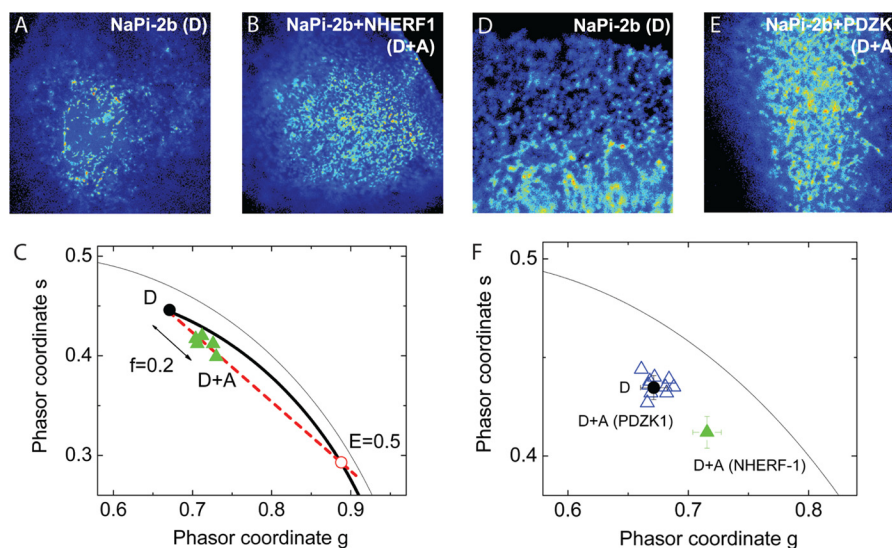


FIGURE 5. **FLIM-FRET studies in CACO-2^{BBE} cells confirmed interaction of NaPi-2b with NHERF1.** CACO-2^{BBE} cells transfected with Cu-NaPi-2b (A) or co-transfected with Cu-NaPi-2b and EYFP-NHERF1 (B) were studied. The phasor diagram showed a displacement of fluorescence lifetime in the cells co-transfected (green triangles) compared with cells transfected only with Cu-NaPi-2b (C). The reduction in donor lifetime fluorescence marks the occurrence of FRET and, therefore that both proteins are within 10 nm. Fluorescence lifetime analysis was repeated for the NaPi-2b/PDZK1 pair (D and E). In this case, there was no significant variation in the fluorescence lifetime of co-transfected cells (blue triangles) compared with the solo transfection of Cu-NaPi-2b (F) meaning no occurrence of FRET. In this phasor diagram, average lifetime of the NaPi-2b/NHERF1 pair (green triangle) is included for comparison (F).

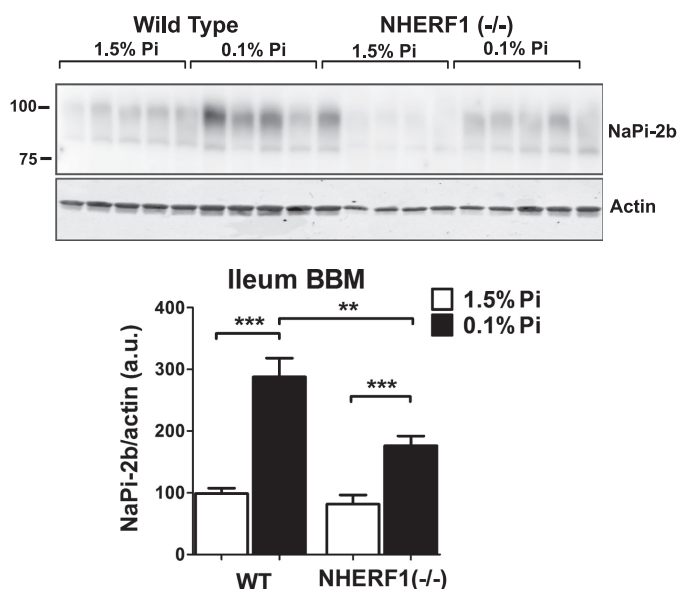


FIGURE 6. **NHERF1 KO mice have impaired adaptation of NaPi-2b protein in response to a low P_i diet.** Mice ileal BBMs were analyzed by Western blot to detect NaPi-2b expression. Wild type animals fed a low P_i diet showed a significant increase on the expression of NaPi-2b compared with animals fed a high P_i diet. However, NHERF1^{-/-} mice had a 39 ± 11% decrease in the adaptive response of NaPi-2b under the same conditions.

elevated P_i excretion in the urine. These changes were paralleled by loss of NaPi-2a in the microvillar membranes of the renal proximal tubule cells, indicating that NHERF1 was playing a pivotal role in retaining NaPi-2a within the apical membrane to permit the reabsorption of filtered P_i from the lumen of the nephron. Following the discovery of the NHERF1/NaPi-2a interaction, other PDZ domain containing proteins, including PDZK1 (also known as NHERF3 or NaPi-Cap1) have also been found to bind to NaPi-2a (19, 21, 49). Discernible in mice maintained on a high P_i diet, PDZK1^{-/-} mice had diminished retention of NaPi-2a within the apical membrane of renal

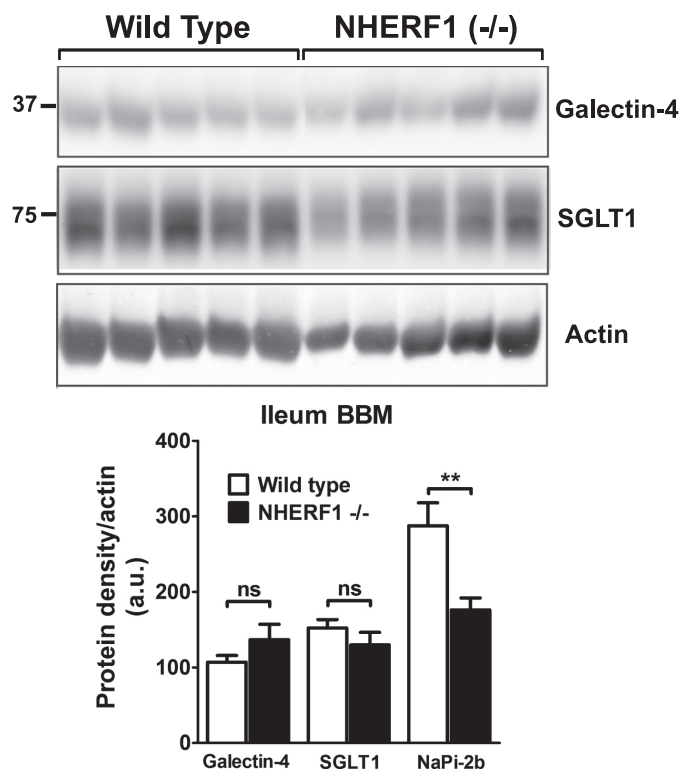


FIGURE 7. **Expression of other apical membrane-associated proteins is not modified in the NHERF1^{-/-} mice.** Western blot analysis of ileal BBM of wild type or NHERF1^{-/-} animals fed low P_i diets. Two apical membrane-associated proteins, Galectin-4 and Na⁺-D-glucose cotransporter (SGLT1), showed no differential expression between wild type and NHERF1^{-/-} animals unlike NaPi-2b that showed a significant reduction in NHERF1^{-/-} mice under this dietary condition (n = 8–10). ns, not significant.

proximal tubule cells but showing a much milder phenotype than NHERF1^{-/-} mice (25). The complimentary roles of NHERF1 and PDZK1 in retaining NaPi-2a within the microvillar membrane of renal proximal tubule cells extended to the

NaPi-2b Transporter Interacts with the PDZ Protein NHERF1

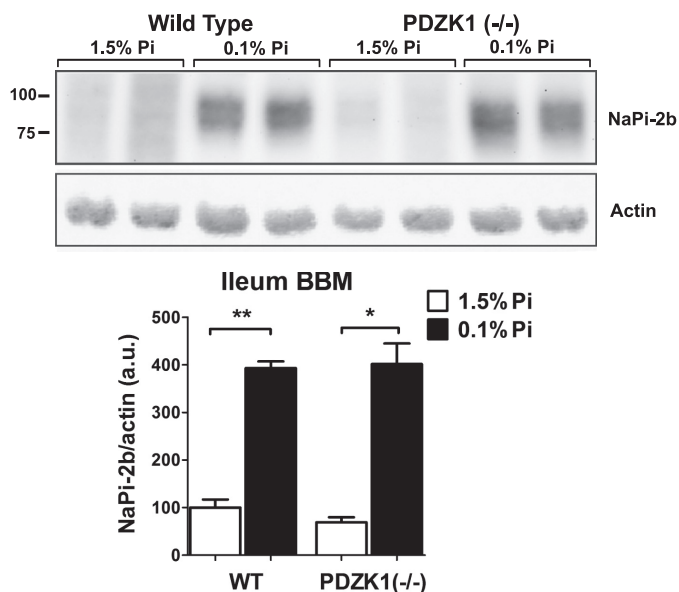


FIGURE 8. PDZK1 KO mice have a normal adaptation to low P_i diet intake. In contrast to the impaired adaptation in the NHERF1^{-/-} mice, wild type and PDZK1^{-/-} mice showed no differences in the adaptive response of NaPi-2b apical expression. Ileal BBMs NaPi-2b levels were increased to the same extent in wild type and PDZK1^{-/-} mice fed a low P_i diet.

regulation of NaPi-2c within the same domain. NaPi-2c is a distinct gene product from NaPi-2a but the two proteins share a high degree of sequence homology and perform sodium-dependent P_i co-transport across the microvillar membrane of renal proximal tubule cells. Despite the absence of a canonical PDZ binding motif at its C terminus, NaPi-2c is also bound by both NHERF1 and PDZK1, however, with preferential binding to PDZK1 (22, 23).

NHERF1 Binds NaPi-2b in Enterocytes—Given the demonstrated role of NHERF1 and PDZK1 in binding and regulating NaPi-2a and NaPi-2c, the present study sought to test the hypothesis that NHERF1 and PDZK1 bound and regulated the third family member, NaPi-2b. Unlike NaPi-2a and NaPi-2c, NaPi-2b is not expressed in renal proximal tubule cells but is expressed in small intestinal enterocytes (50). In enterocytes, NaPi-2b is concentrated within the apical microvilli and is responsible for ~90% of the P_i absorption from the intestinal lumen (10). Sequence analysis of NaPi-2b across species reveals a canonical type I PDZ binding motif at its C-terminal tail (supplemental Fig. S4). Three lines of evidence demonstrated that NaPi-2b was bound by NHERF1. First, NaPi-2b specifically co-precipitated with NHERF1 following the immunoprecipitation of NHERF1 from rat enterocytes. Second, GFP-NaPi-2b specifically co-precipitated with FLAG-NHERF1 when both proteins were coexpressed in HEK cells. This interaction was greatly diminished when the amino acids that comprise the PDZ binding motif on NaPi-2b were truncated from the coding sequence. Third, when CACO₂_{BBE} cells were co-transfected with Cu-NaPi-2b and EYFP-NHERF1 and evaluated by FLIM-FRET there was a substantial decrease in the fluorescence lifetime of the donor fluorophore. This demonstrates the presence of energy transfer between the two fluorophores and indicates that the Cu-NaPi-2b and EYFP-NHERF1 proteins resided within 10 nm of each other. Parallel studies with PDZK1 indi-

cated that NaPi-2b did not co-immunoprecipitate with PDZK1, and there was not FLIM-FRET between Cu-NaPi-2b and EYFP-PDZK1.

NHERF1 Modulates NaPi-2b Abundance in Enterocytes—Mice maintained on a low P_i diet have significantly lower serum P_i levels (51). To minimize the loss of P_i in the urine, these mice increase the abundance of NaPi-2a and NaPi-2c in the microvillar membrane of the renal proximal tubule cells (51, 52). Simultaneously, to maximize the uptake of ingested P_i , these mice increase the abundance of NaPi-2b in the microvillar membrane of the small intestinal enterocytes (13). The molecular mechanisms involved in the increased NaPi-2b abundance have not been well delineated, and could include increases in transcription, translation, and protein retention or decreases in protein turnover. The present studies, however, indicate that NHERF1 impacts the adaptive response of NaPi-2b to low dietary P_i . In the NHERF1 KO mice model the adaptation induced by a low P_i diet of the NaPi-2b transporter was disturbed compared with the wild type animal. NaPi-2b up-regulation in the apical membrane of enterocytes was dramatically reduced in NHERF1 KO mice fed a low P_i diet. In parallel we also studied PDZK1 KO animals adapted to the same dietary conditions. PDZK1 KO animals did not show any differences with wild type animals showing a similar up-regulation of the NaPi-2b transporter in the apical membrane. This effect seems to reflect a more important role of NHERF1 in the stabilization or regulation of the apical expression of the NaPi-2b cotransporters in the small intestine during adaptation to low P_i diets. The results of the *in vivo* models are in accordance to the *in vitro* analysis of the protein interactions of NaPi-2b that demonstrated the binding to NHERF1 but strongly suggested a lack of interaction with the PDZK1 protein.

NHERF Proteins as Modulators of Epithelial Transporters—Although NaPi-2a, NaPi-2b, and NaPi-2c share a high sequence homology, their C-terminal tails differ significantly (supplemental Fig. S4), implying a differential affinity for PDZ proteins. For example, NaPi-2a is able to interact with a numerous group of PDZ proteins besides NHERF-1 and PDZK1, including Shank2E (20, 21), CAL (53), or the other members of the NHERF family (NHERF-2 and -4) (19). In contrast the only proved NaPi-2c interactions are with PDZK1 and NHERF1 (22), with preferential affinity for PDZK1 (23). The present study shows that the NaPi-2b protein binds to the NHERF1 PDZ protein with lack of evidence for PDZK1 interaction. Further studies will be needed to characterize the interactions of NaPi-2b with other PDZ domain containing proteins. These results highlight the differences on the regulatory mechanisms between the three type II NaPi transporters and partially explain their differential response to physiological stimuli.

The precise role of NHERF1 or PDZK1 in the regulation of NaPi transporters is not yet clear although they have been suggested to function in the retention/stability of the transporters in the apical membrane. Other intestinal transporters as Slc15a1 and Slc22a5 are regulated in a similar way by PDZK1 (54). Interestingly, NHERF1 and PDZK1 regulation of other epithelial transporters also involves other regulatory mechanisms. For example, the activity of the cystic fibrosis transmembrane conductance regulator or the NHE3 transporter are

modulated by NHERF1 and PDZK1 through different mechanisms including, trafficking and retention of the transporter, homodimerization or interaction with other transporters, and the formation of multiprotein signaling complexes (33, 55, 56). Most of these mechanisms involve direct interaction of the PDZ domain containing protein with the transporters or, in some cases, with both the transporter and a specific GPCR receptor that can modulate the activity or stability of the transporters.

NHERF1-deficient animals do not show any major histological changes in length or ultrastructure of microvilli in the small intestine (30, 57). Moreover, the expression of other apical brush-border membrane proteins, such as Galectin-4 or Na⁺-D-glucose cotransporter (SGLT1), were not impaired in the NHERF1 KO mice compared with wild type. Taken together, these data suggest that impairment in the adaptation of NaPi-2b to low P_i intake in the NHERF1 KO mice is associated to the direct interaction of the NaPi-2b transporter with NHERF1. In summary, these studies demonstrate that NHERF1 associates with NaPi-2b in enterocytes and partially regulates NaPi-2b adaptation to low P_i dietary intake.

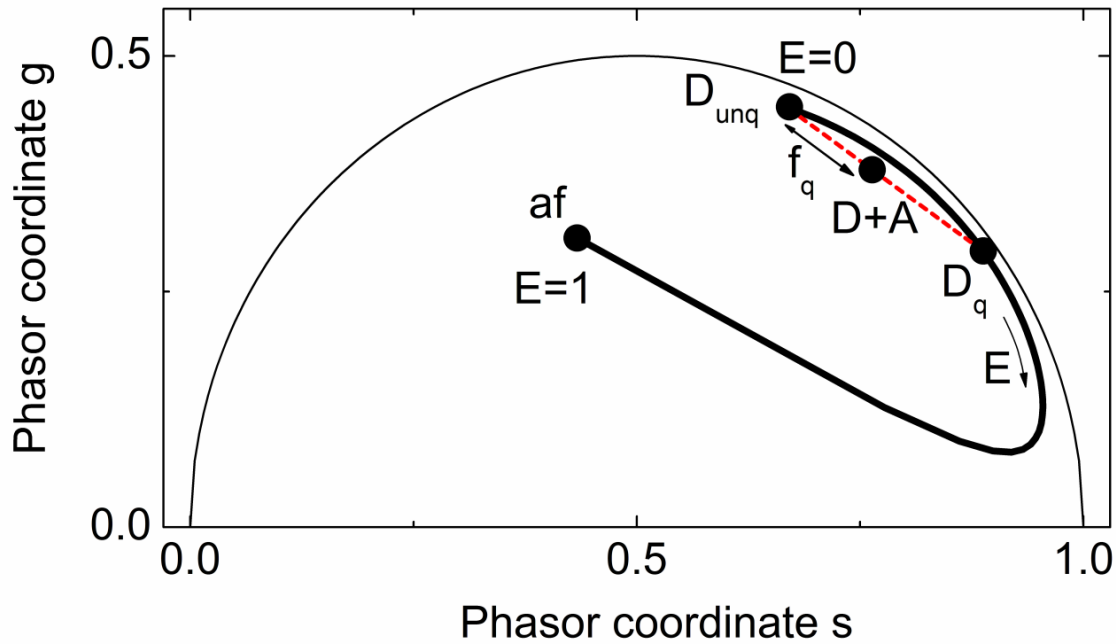
Acknowledgment—We thank Milka Titin for help with preparation of the samples for FLIM-FRET analysis.

REFERENCES

- Berndt, T., and Kumar, R. (2009) Novel mechanisms in the regulation of phosphorus homeostasis. *Physiology* **24**, 17–25
- Alizadeh Naderi, A. S., and Reilly, R. F. (2010) Hereditary disorders of renal phosphate wasting. *Nat. Rev. Nephrol.* **6**, 657–665
- Farrow, E. G., and White, K. E. (2010) Recent advances in renal phosphate handling. *Nat. Rev. Nephrol.* **6**, 207–217
- Tonelli, M., Sacks, F., Pfeffer, M., Gao, Z., and Curhan, G. (2005) Relation between serum phosphate level and cardiovascular event rate in people with coronary disease. *Circulation* **112**, 2627–2633
- Dhingra, R., Sullivan, L. M., Fox, C. S., Wang, T. J., D'Agostino, R. B., Sr., Gaziano, J. M., and Vasan, R. S. (2007) Relations of serum phosphorus and calcium levels to the incidence of cardiovascular disease in the community. *Arch. Intern. Med.* **167**, 879–885
- Shuto, E., Taketani, Y., Tanaka, R., Harada, N., Isshiki, M., Sato, M., Nashiki, K., Amo, K., Yamamoto, H., Higashi, Y., Nakaya, Y., and Takeda, E. (2009) Dietary phosphorus acutely impairs endothelial function. *J. Am. Soc. Nephrol.* **20**, 1504–1512
- Kempson, S. A., Lötscher, M., Kaissling, B., Biber, J., Murer, H., and Levi, M. (1995) Parathyroid hormone action on phosphate transporter mRNA and protein in rat renal proximal tubules. *Am. J. Physiol.* **268**, F784–791
- Segawa, H., Yamanaka, S., Onitsuka, A., Tomoe, Y., Kuwahata, M., Ito, M., Taketani, Y., and Miyamoto, K. (2007) Parathyroid hormone-dependent endocytosis of renal type IIc NaP_i cotransporter. *Am. J. Physiol. Renal Physiol.* **292**, F395–403
- Segawa, H., Kawakami, E., Kaneko, I., Kuwahata, M., Ito, M., Kusano, K., Saito, H., Fukushima, N., and Miyamoto, K. (2003) Effect of hydrolysis-resistant FGF23-R179Q on dietary phosphate regulation of the renal type-II NaP_i transporter. *Pflugers Arch.* **446**, 585–592
- Sabbagh, Y., O'Brien, S. P., Song, W., Boulanger, J. H., Stockmann, A., Arbeen, C., and Schiavi, S. C. (2009) Intestinal npt2b plays a major role in phosphate absorption and homeostasis. *J. Am. Soc. Nephrol.* **20**, 2348–2358
- Marks, J., Srail, S. K., Biber, J., Murer, H., Unwin, R. J., and Debnam, E. S. (2006) Intestinal phosphate absorption and the effect of vitamin D. A comparison of rats with mice. *Exp. Physiol.* **91**, 531–537
- Giral, H., Caldas, Y., Sutherland, E., Wilson, P., Breusegem, S., Barry, N., Blaine, J., Jiang, T., Wang, X. X., and Levi, M. (2009) Regulation of rat intestinal sodium-dependent phosphate transporters by dietary phosphate. *Am. J. Physiol. Renal Physiol.* **297**, F1466–1475
- Hattenhauer, O., Traebert, M., Murer, H., and Biber, J. (1999) Regulation of small intestinal Na-P_i type IIb cotransporter by dietary phosphate intake. *Am. J. Physiol. Gastrointest. Liver Physiol.* **277**, G756–762
- Forster, I. C., Hernando, N., Biber, J., and Murer, H. (2006) Proximal tubular handling of phosphate. A molecular perspective. *Kidney Int.* **70**, 1548–1559
- Miyamoto, K., Ito, M., Tatsumi, S., Kuwahata, M., and Segawa, H. (2007) New aspect of renal phosphate reabsorption. The type IIc sodium-dependent phosphate transporter. *Am. J. Nephrol.* **27**, 503–515
- Nourry, C., Grant, S. G., and Borg, J. P. (2003) PDZ domain proteins. Plug and play! *Sci. STKE* **2003**, RE7
- Sugiura, T., Shimizu, T., Kijima, A., Minakata, S., and Kato, Y. (2011) PDZ adaptors. Their regulation of epithelial transporters and involvement in human diseases. *J. Pharm. Sci.* **100**, 3620–3635
- Lee, H. J., and Zheng, J. J. (2010) PDZ domains and their binding partners. Structure, specificity, and modification. *Cell Commun. Signal.* **8**, 8
- Gisler, S. M., Stajlar, I., Traebert, M., Bacic, D., Biber, J., and Murer, H. (2001) Interaction of the type IIa Na/P_i cotransporter with PDZ proteins. *J. Biol. Chem.* **276**, 9206–9213
- Dobrinskikh, E., Giral, H., Caldas, Y. A., Levi, M., and Doctor, R. B. (2010) Shank2 redistributes with NaP_i during regulated endocytosis. *Am. J. Physiol. Cell Physiol.* **299**, C1324–1334
- McWilliams, R. R., Breusegem, S. Y., Brodsky, K. F., Kim, E., Levi, M., and Doctor, R. B. (2005) Shank2E binds NaP_i cotransporter at the apical membrane of proximal tubule cells. *Am. J. Physiol. Cell Physiol.* **289**, C1042–1051
- Villa-Bellosta, R., Barac-Nieto, M., Breusegem, S. Y., Barry, N. P., Levi, M., and Sorribas, V. (2008) Interactions of the growth-related, type IIc renal sodium/phosphate cotransporter with PDZ proteins. *Kidney Int.* **73**, 456–464
- Giral, H., Lanzano, L., Caldas, Y., Blaine, J., Verlander, J. W., Lei, T., Gratton, E., and Levi, M. (2011) Role of PDZK1 protein in apical membrane expression of renal sodium-coupled phosphate transporters. *J. Biol. Chem.* **286**, 15032–15042
- Shenolikar, S., Voltz, J. W., Minkoff, C. M., Wade, J. B., and Weinman, E. J. (2002) Targeted disruption of the mouse *NHERF-1* gene promotes internalization of proximal tubule sodium-phosphate cotransporter type IIa and renal phosphate wasting. *Proc. Natl. Acad. Sci. U.S.A.* **99**, 11470–11475
- Capuano, P., Bacic, D., Stange, G., Hernando, N., Kaissling, B., Pal, R., Kocher, O., Biber, J., Wagner, C. A., and Murer, H. (2005) Expression and regulation of the renal Na/phosphate cotransporter NaP_i-IIa in a mouse model deficient for the PDZ protein PDZK1. *Pflugers Arch.* **449**, 392–402
- Lan, D., and Silver, D. L. (2005) Fenofibrate induces a novel degradation pathway for scavenger receptor B-I independent of PDZK1. *J. Biol. Chem.* **280**, 23390–23396
- Caldas, Y. A., Giral, H., Cortazar, M. A., Sutherland, E., Okamura, K., Blaine, J., Sorribas, V., Koepsell, H., and Levi, M. (2011) Liver X receptor-activating ligands modulate renal and intestinal sodium-phosphate transporters. *Kidney Int.* **80**, 535–544
- Peterson, M. D., and Mooseker, M. S. (1992) Characterization of the enterocyte-like brush border cytoskeleton of the C2BB6 clones of the human intestinal cell line, Caco-2. *J. Cell Sci.* **102**, 581–600
- Colyer, R. A., Lee, C., and Gratton, E. (2008) A novel fluorescence lifetime imaging system that optimizes photon efficiency. *Microsc. Res. Tech.* **71**, 201–213
- Broere, N., Chen, M., Cinar, A., Singh, A. K., Hillesheim, J., Riederer, B., Lünemann, M., Rottinghaus, I., Krabbenhöft, A., Engelhardt, R., Rausch, B., Weinman, E. J., Donowitz, M., Hubbard, A., Kocher, O., de Jonge, H. R., Hogema, B. M., and Seidler, U. (2009) Defective jejunal and colonic salt absorption and altered Na⁺/H⁺ exchanger 3 (NHE3) activity in NHE regulatory factor 1 (NHERF1) adaptor protein-deficient mice. *Pflugers Arch.* **457**, 1079–1091
- Redford, G. I., and Clegg, R. M. (2005) Polar plot representation for frequency-domain analysis of fluorescence lifetimes. *J. Fluoresc.* **15**, 805–815
- Lanzano, L., Digman, M. A., Fwu, P., Giral, H., Levi, M., and Gratton, E.

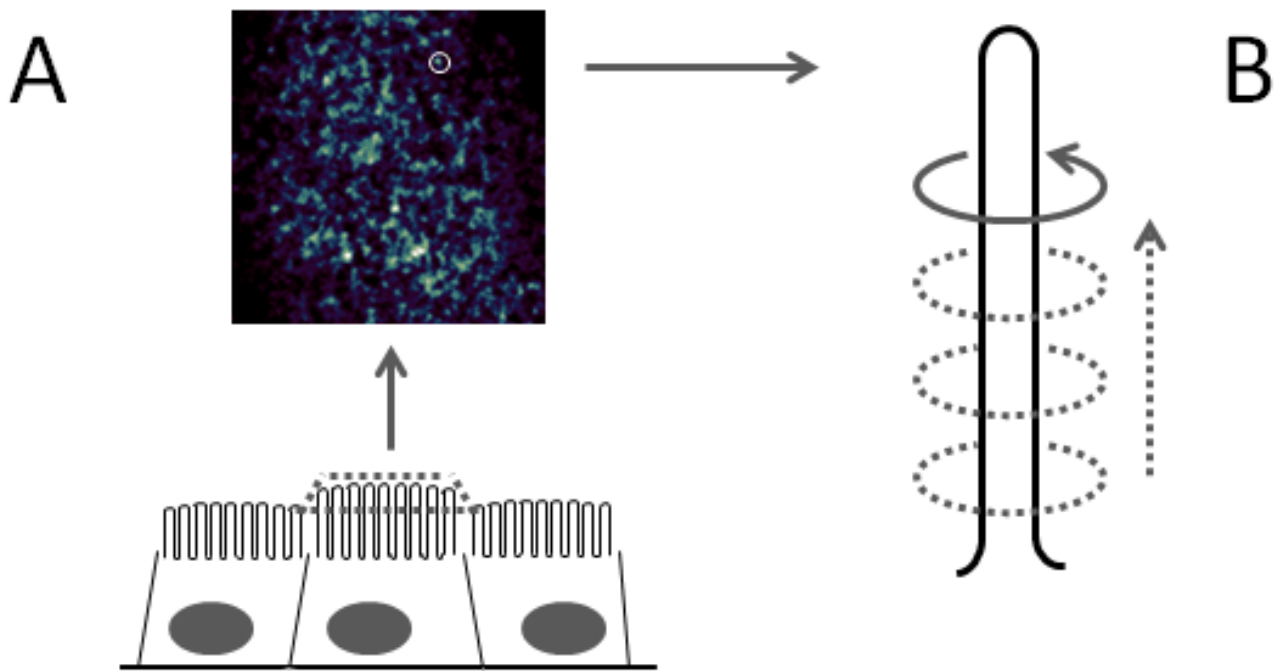
- (2011) Nanometer-scale imaging by the modulation tracking method. *J. Biophotonics* **4**, 415–424
33. Lamprecht, G., and Seidler, U. E. (1998) The emerging role of PDZ adapter proteins for regulation of intestinal ion transport. *J. Biol. Chem.* **273**, 29972–29978
 34. Musch, M. W., Lucioni, A., and Chang, E. B. (2008) Aldosterone regulation of intestinal Na absorption involves SGK-mediated changes in NHE3 and Na⁺ pump activity. *Am. J. Physiol. Gastrointest. Liver Physiol.* **295**, G909–919
 35. Zachos, N. C., Li, X., Kovbasnjuk, O., Hogema, B., Sarker, R., Lee, L. J., Li, M., de Jonge, H., and Donowitz, M. (2009) NHERF3 (PDZK1) contributes to basal and calcium inhibition of NHE3 activity in Caco-2BBE cells. *J. Biol. Chem.* **284**, 23708–23718
 36. Lin, R., Murtazina, R., Cha, B., Chakraborty, M., Sarker, R., Chen, T. E., Lin, Z., Hogema, B. M., de Jonge, H. R., Seidler, U., Turner, J. R., Li, X., Kovbasnjuk, O., and Donowitz, M. (2011) D-Glucose acts via sodium/glucose cotransporter 1 to increase NHE3 in mouse jejunal brush border by a Na⁺/H⁺ exchange regulatory factor 2-dependent process. *Gastroenterology* **140**, 560–571
 37. Fujiya, M., Inaba, Y., Musch, M. W., Hu, S., Kohgo, Y., and Chang, E. B. (2011) Cytokine regulation of OCTN2 expression and activity in small and large intestine. *Inflamm. Bowel Dis.* **17**, 907–916
 38. Peterson, M. D., Bement, W. M., and Mooseker, M. S. (1993) An *in vitro* model for the analysis of intestinal brush border assembly. II. Changes in expression and localization of brush border proteins during cell contact-induced brush-border assembly in Caco-2BBE cells. *J. Cell Sci.* **105**, 461–472
 39. Peterson, M. D., and Mooseker, M. S. (1993) An *in vitro* model for the analysis of intestinal brush-border assembly. I. Ultrastructural analysis of cell contact-induced brush-border assembly in Caco-2BBE cells. *J. Cell Sci.* **105**, 445–460
 40. Digman, M. A., Caiola, V. R., Zamai, M., and Gratton, E. (2008) The phasor approach to fluorescence lifetime imaging analysis. *Biophys. J.* **94**, L14–16
 41. Capuano, P., Radanovic, T., Wagner, C. A., Bacic, D., Kato, S., Uchiyama, Y., St-Arnoud, R., Murer, H., and Biber, J. (2005) Intestinal and renal adaptation to a low-P_i diet of type II NaP_i cotransporters in vitamin D receptor- and 1 α OHase-deficient mice. *Am. J. Physiol. Cell Physiol.* **288**, C429–434
 42. Hung, A. Y., and Sheng, M. (2002) PDZ domains. Structural modules for protein complex assembly. *J. Biol. Chem.* **277**, 5699–5702
 43. Weinman, E. J., Steplock, D., and Shenolikar, S. (1993) CAMP-mediated inhibition of the renal brush-border membrane Na⁺-H⁺ exchanger requires a dissociable phosphoprotein cofactor. *J. Clin. Invest.* **92**, 1781–1786
 44. Reczek, D., Berryman, M., and Bretscher, A. (1997) Identification of EBP50. A PDZ-containing phosphoprotein that associates with members of the ezrin-radixin-moesin family. *J. Cell Biol.* **139**, 169–179
 45. Weinman, E. J., Steplock, D., Wang, Y., and Shenolikar, S. (1995) Characterization of a protein cofactor that mediates protein kinase A regulation of the renal brush-border membrane Na⁺-H⁺ exchanger. *J. Clin. Invest.* **95**, 2143–2149
 46. Hall, R. A., Ostedgaard, L. S., Premont, R. T., Blitzer, J. T., Rahman, N., Welsh, M. J., and Lefkowitz, R. J. (1998) A C-terminal motif found in the β_2 -adrenergic receptor, P2Y1 receptor and cystic fibrosis transmembrane conductance regulator determines binding to the Na⁺/H⁺ exchanger regulatory factor family of PDZ proteins. *Proc. Natl. Acad. Sci. U.S.A.* **95**, 8496–8501
 47. Hegedüs, T., Sessler, T., Scott, R., Thelin, W., Bakos, E., Váradi, A., Szabó, K., Homolya, L., Milgram, S. L., and Sarkadi, B. (2003) C-terminal phosphorylation of MRP2 modulates its interaction with PDZ proteins. *Biochem. Biophys. Res. Commun.* **302**, 454–461
 48. Weinman, E. J., Boddeti, A., Cunningham, R., Akom, M., Wang, F., Wang, Y., Liu, J., Steplock, D., Shenolikar, S., and Wade, J. B. (2003) NHERF-1 is required for renal adaptation to a low-phosphate diet. *Am. J. Physiol. Renal Physiol.* **285**, F1225–1232
 49. Biber, J., Gisler, S. M., Hernando, N., and Murer, H. (2005) Protein/protein interactions (PDZ) in proximal tubules. *J. Membr. Biol.* **203**, 111–118
 50. Hilfiker, H., Hattenhauer, O., Traebert, M., Forster, I., Murer, H., and Biber, J. (1998) Characterization of a murine type II sodium-phosphate cotransporter expressed in mammalian small intestine. *Proc. Natl. Acad. Sci. U.S.A.* **95**, 14564–14569
 51. Hoag, H. M., Martel, J., Gauthier, C., and Tenenhouse, H. S. (1999) Effects of *Npt2* gene ablation and low-phosphate diet on renal Na⁺/phosphate cotransport and cotransporter gene expression. *J. Clin. Invest.* **104**, 679–686
 52. Ohkido, I., Segawa, H., Yanagida, R., Nakamura, M., and Miyamoto, K. (2003) Cloning, gene structure, and dietary regulation of the type-IIc Na/Pi cotransporter in the mouse kidney. *Pflugers Arch.* **446**, 106–115
 53. Lanaspá, M. A., Giral, H., Breusegem, S. Y., Halaihel, N., Baile, G., Catalán, J., Carrodegua, J. A., Barry, N. P., Levi, M., and Sorribas, V. (2007) Interaction of MAP17 with NHERF3/4 induces translocation of the renal Na/Pi Ila transporter to the trans-Golgi. *Am. J. Physiol. Renal Physiol.* **292**, F230–242
 54. Sugiura, T., Kato, Y., Wakayama, T., Silver, D. L., Kubo, Y., Iseki, S., and Tsuji, A. (2008) PDZK1 regulates two intestinal solute carriers (Slc15a1 and Slc22a5) in mice. *Drug Metab. Dispos.* **36**, 1181–1188
 55. Singh, A. K., Riederer, B., Krabbenhoft, A., Rausch, B., Bonhagen, J., Lehmann, U., de Jonge, H. R., Donowitz, M., Yun, C., Weinman, E. J., Kocher, O., Hogema, B. M., and Seidler, U. (2009) Differential roles of NHERF1, NHERF2, and PDZK1 in regulating CFTR-mediated intestinal anion secretion in mice. *J. Clin. Invest.* **119**, 540–550
 56. Broere, N., Hillesheim, J., Tuo, B., Jorna, H., Houtsmuller, A. B., Shenolikar, S., Weinman, E. J., Donowitz, M., Seidler, U., de Jonge, H. R., and Hogema, B. M. (2007) Cystic fibrosis transmembrane conductance regulator activation is reduced in the small intestine of Na⁺/H⁺ exchanger 3 regulatory factor 1 (NHERF-1)- but not NHERF-2-deficient mice. *J. Biol. Chem.* **282**, 37575–37584
 57. Donowitz, M., Singh, S., Singh, P., Salahuddin, F. F., Chen, Y., Chakraborty, M., Murtazina, R., Gucek, M., Cole, R. N., Zachos, N. C., Kovbasnjuk, O., Broere, N., Smalley-Freed, W. G., Reynolds, A. B., Hubbard, A. L., Seidler, U., Weinman, E., de Jonge, H. R., Hogema, B. M., and Li, X. (2010) Alterations in the proteome of the NHERF1 knockout mouse jejunal brush-border membrane vesicles. *Physiol. Genomics* **42A**, 200–210

Supplementary figure 1



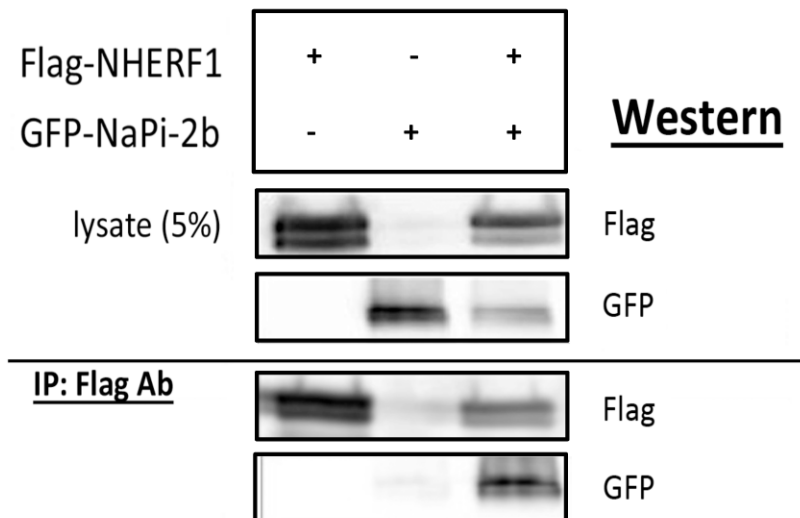
Supplementary Figure 1. Representative diagram of phasor approach and calculations of FRET efficiency and fraction of interacting donors. Frequency-domain lifetime measurements at each of the pixels of an image resulted in a value of the modulation and phase that were used to determine the radial and angular coordinates in the phasor plot. The phasor associated to each image was determined as the average phasor of the pixels corresponding to the cell apical membrane and the phasor of the autofluorescence (af) was determined by imaging non-transfected cells. For each experiment, the unquenched donor (D_{unq}) and the af phasor have been determined and a trajectory between them has been calculated (solid line). This trajectory represent the FRET efficiency (E) varying from $E=0$ at the D_{unq} position to $E=1$ at the af phasor position. Any phasor along this trajectory corresponds to pure species of donor quenched (D_q) with FRET efficiency E . However, in a given experiment each pixel may contain a mixture of quenched and unquenched donors with relative fractions f_q and f_{unq} respectively. In order to quantify FRET results we analyzed the shift of the phasor of the donor in presence of the acceptor with respect to the donor only and we can trace a segment (dashed line) from the only donor (D_{unq}) to the donor + acceptor (D+A) phasors that will also intersect with the efficiency trajectory. This intersection point is used to calculate the FRET efficiency (E) since this point represents the maximum FRET detectable if all the donors were ideally paired with an acceptor (D_q). Moreover, we can also calculate the fraction of donors undergoing FRET (f_q) from the distance of the phasor D+A from D_{unq} divided by the length of the entire segment.

Supplementary figure 2



Supplementary Figure 2. Schematic representation of the Modulation Tracking (MT) imaging method. **A)** First a raster scan is performed with the confocal microscope to localize the microvilli at the apical membrane. One isolated microvillus is selected and the scanner is pointed on its coordinates. **B)** The selected microvillus is tracked by scanning the laser spot in circular orbits around the microvilli. A single particle tracking algorithm based on the calculation of the Fast Fourier Transform (FFT) of the intensity along the orbit is used to keep the microvillus always at the center of the scanned orbit. The position of the microvillus is tracked while scanning at different sections along its length to obtain a 3D image of the microvillar surface. The orbit period is set to 8ms and the position of the center of the scanning orbit is updated every 64ms, a time resolution sufficient to follow the relatively slow movements of the microvillus. The final 3D reconstruction of the microvilli surface is painted in color scale according to the fluorescence intensity recorded in one channel (Figure 4).

Supplementary Figure 3



Supplementary Figure 3. GFP-NaPi-2b co-precipitates with Flag-NHERF1. HEK cells were transfected with Flag-NHERF1, GFP-NaPi-2b or both constructs. In the upper panel, Western blotting of the total lysates demonstrates the fusion proteins are appropriately expressed. In the lower panel, following Flag co-precipitation, Western blotting showed GFP-NaPi-2b was co-precipitated when cells were co-transfected with Flag-NHERF1.

Supplementary figure 4

A

Class I	-X-	S/T	-X-	φ
Class II	-X-	φ	-X-	φ
Class III	-X-	D/E	-X-	φ

φ- hydrophobic residue
X- any residue

Mouse NaPi-2b (691)	LSNTTVF	Rodents
Rat NaPi-2b (689)	LSNTTVF	
Human NaPi-2b (684)	KTECTAL	Primates
Orangutan NaPi-2b (683)	KTECTAL	
Sumatran orangutan NaPi-2b (683)	KTECTAL	
Chimpanzee NaPi-2b (685)	KTECTAL	
Callithrix jacchus NaPi-2b (684)	KTECTAL	Mammals
Cattle NaPi-2b (687)	VSSVTAL	
Water buffalo NaPi-2b (687)	VSSVTAL	
Dog NaPi-2b (688)	MSGSTAL	
Giant panda NaPi-2b (687)	TSSSTAL	
Chicken NaPi-2b (668)	GTNNTAL	
Catfish NaPi-2b (615)	ILNVTAL	
Zebrafish NaPi-2b (625)	ILKATSL	
Xenopus NaPi-2b (668)	SQLNTSF	
Consensus	IS TAL	

Mouse- *Mus musculus*, NP_035532.2; Rat- *Rattus norvegicus*, NP_445832.1; Human- *Homo sapiens*, AAI46667.1; Orangutan- *Pongo pygmaeus*, Q5REV9; Sumatran orangutan- *Pongo abelii*, NP_001124770; Chimpanzee- *Pan troglodytes*, XP_003310312; *Callithrix jacchus*, XP_002745982; Cattle- *Bos Taurus*, Q27960; Water buffalo- *Bubalus bubalis*, ADW66550; Dog, *Canis lupus familiaris*, XP_545968; Giant panda- *Ailuropoda melanoleuca*, XP_002924589; Chicken- *Gallus gallus*, NP_989805; Catfish- *Pelteobagrus fulvidraco*- ADM18964; Zebrafish- *Danio rerio*, NP_571699; Xenopus- *Xenopus laevis*, NP_989302.

B

Species	CFTR	NHE3	NaPi-2a	NaPi-2b	NaPi-2c
Human	-D-T-R-L	-S-T-H-M	-A-T-R-L	-C-T-A-L	-S-Q-Q-L
Mouse	-E-T-R-L	-S-T-H-M	-A-T-R-L	-T-T-V-F	-S-Q-Q-L
Rat	-E-T-R-L	-S-T-H-M	-A-T-R-L	-T-T-V-F	-S-Q-Q-L

Supplementary Figure 4. Evolutionary conservation of NaPi-2b putative PDZ-binding site at its C-terminus. **A)** Comparison of NaPi-2b protein sequences from different species were performed by ClustalW alignment analysis. The alignment of the last 7 amino acids on the C-terminal tail of 15 different species is shown. All the sequences analyzed fitted on the class I PDZ-binding motif consensus. Sequence accession numbers have been included below the table. **B)** The 4 last amino acids of the C-terminal tails of different epithelial transporters are shown in the table. Most of these transporters present also a class I PDZ-binding motif including CFTR, NHE3, NaPi-2a and NaPi-2b. The exception is NaPi-2c transporter that contains a sequence that is not perfectly matching with any of the described consensus motifs.

NHE3 Regulatory Factor 1 (NHERF1) Modulates Intestinal Sodium-dependent Phosphate Transporter (NaPi-2b) Expression in Apical Microvilli

Hector Giral, DeeAnn Cranston, Luca Lanzano, Yupanqui Caldas, Eileen Sutherland, Joanna Rachelson, Evgenia Dobrinskikh, Edward J. Weinman, R. Brian Doctor, Enrico Gratton and Moshe Levi

J. Biol. Chem. 2012, 287:35047-35056.

doi: 10.1074/jbc.M112.392415 originally published online August 17, 2012

Access the most updated version of this article at doi: [10.1074/jbc.M112.392415](https://doi.org/10.1074/jbc.M112.392415)

Alerts:

- [When this article is cited](#)
- [When a correction for this article is posted](#)

[Click here](#) to choose from all of JBC's e-mail alerts

Supplemental material:

<http://www.jbc.org/content/suppl/2012/08/17/M112.392415.DC1.html>

This article cites 57 references, 29 of which can be accessed free at <http://www.jbc.org/content/287/42/35047.full.html#ref-list-1>